Author/s:
Piacentino, EL;Rodriguez, E;Parker, K;Gilbert, TM;O'Hair, RAJ;Ryzhov, V

Title:
Gas-phase functionalized carbon-carbon coupling reactions catalyzed by Ni (II) complexes

Date:
2019-06-01

Citation:
Piacentino, E. L., Rodriguez, E., Parker, K., Gilbert, T. M., O'Hair, R. A. J. & Ryzhov, V. (2019). Gas-phase functionalized carbon-carbon coupling reactions catalyzed by Ni (II) complexes. Journal of Mass Spectrometry, 54 (6), pp.520-526. https://doi.org/10.1002/jms.4360.

Persistent Link:
https://hdl.handle.net/11343/285893

Ryzhov Victor (Orcid ID: 0000-0001-6041-9821)

Gas-phase functionalized carbon-carbon coupling reactions catalyzed by Ni(II) complexes.

Elettra Piacentino[1], Edwin Rodrigues[1], Kevin Parker[1], Thomas M. Gilbert[1], Richard A. J. O'Hair*[2] and Victor Ryzhov*[1#]

[1] Department of Chemistry and Biochemistry, Northern Illinois University, DeKalb, IL 60115, USA

[2] Bio 21 Institute and School of Chemistry, University of Melbourne, Melbourne, Victoria, 3010, Australia

* Corresponding authors.

e-mail: ryzhov@niu.edu; rohair@unimelb.edu.au

[#] Dedicated to Prof. Catherine Fenselau in celebration of her seminal contributions to bioanalytical mass spectrometry and in deep appreciation of her mentorship and guidance.

Keywords: C-C coupling; Ni(II) catalysis; ion-molecule reactions; decarboxylation

Abstract

Gas-phase C-C coupling reactions mediated by Ni(II) complexes were studied using a linear quadrupole ion trap mass spectrometer. Ternary nickel cationic carboxylate complexes, $[(phen)Ni(OOCR^1)]^+$ (where phen = 1,10-phenanthroline) were formed by electrospray ionization. Upon collision-induced dissociation (CID), they extrude CO_2 forming the organometallic cation $[(phen)Ni(R^1)]^+$, which undergoes gas-phase ion-molecule reactions (IMR) with acetate esters CH_3COOR^2 to yield the acetate complex $[(phen)Ni(OOCCH_3)]^+$ and a C-C coupling product R^1-R^2. These Ni(II)-phenanthroline mediated coupling reactions can be performed with a variety of carbon substituents R^1 and R^2 (sp^3, sp^2, or aromatic), some of them functionalized. Reaction rates do not seem to be strongly dependent on the nature of the substituents, as sp^3 - sp^3 or sp^2- sp^2 coupling reactions proceed rapidly. Experimental results are supported by density functional theory calculations, which provide insights into the energetics associated with the C-C bond coupling step.

Introduction

Modern organic synthesis relies heavily on palladium-catalyzed cross-coupling reactions for the construction of C–X bonds (where X = C, N, O, F etc.).[1] Due to the cost of Pd, there is an economic imperative to develop alternative metal catalysts as reflected in the resurgence of interest in the organometallic chemistry of nickel.[2]

Gas-phase studies employing mass spectrometry (MS)-based techniques in conjunction with DFT calculations provide a powerful way of exploring how the electronic structure of the metal, organic group, auxiliary ligand(s), stoichiometry and charge of organometallic complexes influences their fundamental reactivity .[3-8]

Previous studies have revealed that the Pesci reaction provides access to a wide range of organometallic cations and anions via the collision-induced-dissociation (CID) loss of CO_2 from appropriate precursor metal carboxylate complexes (eq. 1a) .[9] When this step is combined with a C-C bond coupling step involving an ester (eq. 1b), a catalytic cycle can be closed for the CO_2ExR (Extrusion-Recombination) class of reaction (eq. 2).[10]

$$[(L)M^{2+}\ ^{-}OOCR^{1}]^{+} \rightarrow [(L)MR^{1}]^{+} + CO_2 \quad (1a)$$

$$[(L)MR^{1}]^{+} + R^{1}COOR^{2} \rightarrow [(L)M^{2+}\ ^{-}OOCR^{1}]^{+} + R^{1}\text{-}R^{2} \quad (1b)$$

$$R^{1}COOR^{2} \rightarrow R^{1}\text{-}R^{2} + CO_2 \quad (2)$$

Such an approach has been applied to the group 10 transition metals ions $[(phen)M(R)]^+$ ligated by 1,10-phenanthroline and methyl group (R = Me) reacting with allyl acetate to complete the C-C coupling catalytic cycle shown in Scheme 1.[11] Of the various group 10 metals studied, nickel

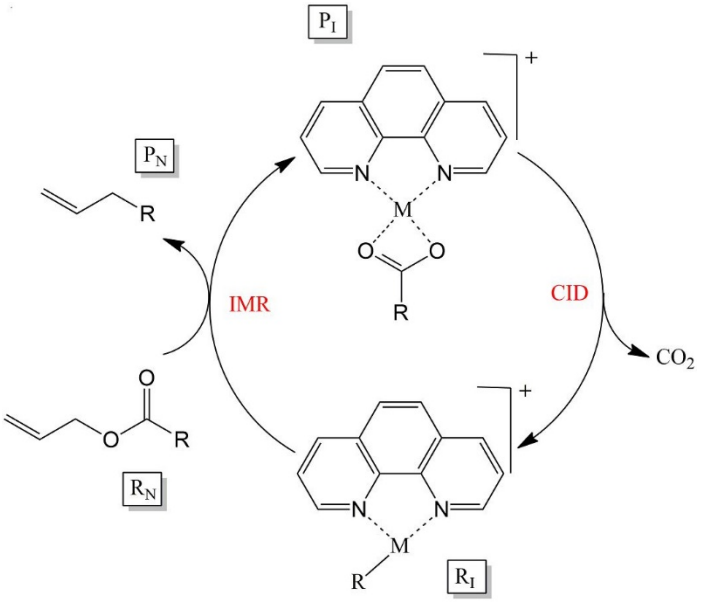

Scheme 1. Two step catalytic cycle for the gas-phase CO_2ExR C-C coupling reaction involving CID loss of CO_2 (eq. 1a) followed by IMR with the ester (eq. 1b).

has lower M-C bond dissociation energy (BDE) than Pd or Pt [2] which results in the higher rate[12] of the second step of the CO_2ExR reaction (eq. 1b). In addition, Ni is over 50 and 300 times less expensive than Pd and Pt, respectively.[2] Given that the previous study was limited to allyl acetate,[9] here we explore a range of other substituted acetate esters as neutral reactants for ion-molecule reactions with a range of other $[(phen)M(R)]^+$ complexes.

Experimental

Materials

Nickel acetate, 1,10-phenanthroline (phen), acetic acid, benzoic acid, acrylic acid and mono- and tri-halogen substituted acetates along with the volatile neutral reactants vinyl acetate, allyl acetate, 2-hydroxyethyl acetate, and 4-methoxybenzyl acetate were all purchased from Sigma-Aldrich (St. Louis, MO, USA) and used as received. Samples were prepared by mixing equal volumes of Ni(O$_2$CCH$_3$)$_2$ (5 mM) and stock solutions of the auxiliary ligand (1 mg/mL). A volume of the carboxylic acids equal to 10% of the nickel/ligand solution volume was then added to the mixture. The sample was allowed to react for 10 min. to assure the formation of the precursor ion and then diluted to a final complex concentration of 0.1 mM with methanol. Solutions prepared with this method were directly injected into the mass spectrometer through an electrospray ion source.

Methods

Mass spectrometry

Mass spectra were obtained using a ThermoFisher linear trap quadrupole mass spectrometer (Thermo Electron, San Jose, USA) custom modified to perform ion molecule reactions (IMR); the modification consists in a bypass line on the instrument helium line. Between the helium tank and the instrument, the helium flow is split in two pathways; while one of the pathways allows for pure helium to reach the ion trap, the other is connected to a membrane fitting where the liquid neutral is injected via syringe pump at the flow rate of 0.01 mL/h and carried into the MS by the He flow.[13] The samples were introduced via ESI to the mass spectrometer at a flow rate of 3.0 μL/min.

Source parameters were set to 12 PSI, 4.0kV for the nebulizer pressure and the needle voltage, respectively, and the source temperature was maintained at 250 ^{0}C. The precursor ion was isolated using windows of about 1 m/z and the fragmentation amplitudes ranged from 10 to 40 N.C.E. Fragmentation was optimized in each case to maximize the product ion signal while ensuring that about 10 % of the precursor ion remained visible. The neutral vapours of allyl acetate, vinyl acetate, 2-hydroxymethyl acetate, and 4-methoxybenzyl acetate were introduced into the ion trap through the helium delivery line, the neutral flow was set for all the neutral reactant used in this study at 0.01 mL/h through a syringe pump. The reaction time was varied by changing the scan delay in the range of 30-1500 ms.

Computational methods

DFT calculations were performed at the M06L/6-311+G(d,p) and at M11L/cc-pVDZ level of theory[14] using Gaussian 09.[15]

The lowest energy conformers and geometry optimization was performed for the three carboxylate complexes $[(phen)Ni(II)(OOCR)]^+$ (where R = acetate, benzoate, acrylate), for all the organometallic products of decarboxylation, $[(phen)Ni(II)(R)]^+$, and for the products of ion-molecule reactions at the M11L/cc-pVDZ level of theory. The subscripts "I" and "N" are used to designate ionic and neutral species respectively. The species associated with the IMR reaction are $(R_I) + (R_N)$, $(R_I + R_N)$, $(P_I) + (P_N)$ and $(P_I + P_N)$, where R and P stand for reactant and product species, respectively. Atomic coordinates for all calculated geometries are given in the supplemental information.

Geometry optimizations were performed on the lowest energy conformers of the carboxylate complexes $[(phen)Ni(R)]^+$, and $[(phen)Ni(OOCR)]^+$, were calculated for both the singlet and the

triplet spin state at the M06L/6-311+G(d,p) level. Both M06L and M11L methods have been successfully used to computationally characterize Ni(II) complexes.[16]

Vibrational frequencies at all levels were computed for each of the structure to ensure that the structure was either a minimum (no imaginary frequencies) or a transition state (one imaginary frequency), and to provide thermodynamic corrections to the electronic energies.

Results and Discussion

Formation of organonickel species via decarboxylation

Ternary carboxylate-phenanthroline-nickel (II) complexes $[(phen)Ni(OOCR)]^+$ are readily formed by ESI as described previously.[11] The three types of carboxylate ligands containing

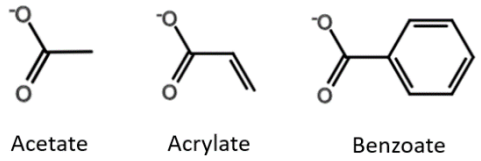

Scheme 2. Structures of the carboxylates used in this work.

sp^3(acetate), sp^2(acrylate), or aromatic (benzoate) substituents are shown in Scheme 2.

CID of these mass-selected complexes resulted in clean decarboxylation (see Fig. 1a for example). This leads to the formation of organonickel ions $[(phen)Ni(R)]^+$ (Scheme 1) where R is an anion binding through the nickel through an sp^3, sp^2, or aromatic carbon substituent. Calculated structures of the three organonickel species are shown in Fig. 2.

All three optimized geometries show distortions from trigonal planar orientations. In the case of $[(phen)Ni(CH_3)]^+$ (a), the distortion appears to arise from a desire of the d8 complex to adopt the classic square planar geometry.[17,18,19] The "cis" C(methyl)-Ni-N angle is 98.9°, while the "trans" C(methyl)-Ni-N angle is 174.3°.

The vinyl (b) and phenyl (c) complexes exhibit agostic [20,21]–interactions in addition to the "square planar" distortion. A hydrocarbon substituent C-H bond acts as a Lewis base toward the

electron-deficient, Lewis acidic nickel ion as a means of increasing the metal's electronic saturation; the interaction is characterized as a two-electron, three-center interaction. For the vinyl complex, the Ni-H distance is 1.656 Å, only slightly longer than the expected Ni-H bond distance (1.6 A). The Ni-C(agostic) distance is 2.029 Å, only 0.2 Å longer than the Ni-C(vinyl) bond distance of 1.808 Å. As a result, the distance from the nickel to the approximate midpoint of the C-H bond is 1.86 Å, a value consistent with those of experimentally observed agostic interactions.[20,21] This is further supported by the lengthening of the C-H bond to 1.159 Å, 0.07 Å more than expected for a C(sp^2)-H bond distance. All of this translates to significant compression of the C(agostic)-C(vinyl)-Ni angle to 79.9°.

Finally, the coplanarity of the vinyl fragment and the Ni(phen) moiety further suggest the presence of the metal/ C-H interaction. For the phenyl complex, the Ni-H distance is 1.776 Å and the Ni-C(agostic) distance is 2.056 Å, meaning the Ni-CH midpoint distance = 1.87 Å. The C-H distance is 1.130 Å and the C(agostic)-C(phenyl)-Ni angle is 80.0°. As for the vinyl, the phenyl and Ni(phen) fragments are coplanar.

All these data support describing the interaction in both complexes as agostic. That the phenomenon does not occur in the methyl complex appears to result from the extreme distortion that would be required to properly orient a methyl C-H bond in proximity to the nickel. Tests suggest that the H-Ni angle would need to compress to < 60° in order to fix the Ni-H distance to 1.7 Å. This compression is likely too endergonic to allow an agostic interaction, even though the nickel cation is sizably Lewis-acidic.

We also examined whether decarboxylation occurs for a variety of halogen-substituted carboxylates of general formula $[(phen)Ni(OOCR)]^+$ (where R = CH_2X or CX_3, and X = F, Cl, Br, or I). Unfortunately CID experiments revealed that instead of decarboxylation occurring, all of these complexes fragmented to produce $[(phen)Ni(X)]^+$ as the sole CID product (data not

shown). These reactions are likely to proceed via similar C-X bond activation mechanisms found for losses of CF_2CO_2 from the coinage metal trifluoroacetates, $[(CF_3CO_2)_2M]^-$ (where M = Cu, Ag and Au).[22]

Ion-molecule reactions of organonickel complexes with esters

The organonickel species $[(phen)Ni(R)]^+$ were reacted with four esters, Scheme 3. We chose four acetate esters CH_3COOR' with various R' groups. Allyl acetate has become almost a "standard" reagent in gas-phase C-C coupling reactions [23-24] and depending on the mechanism provides either a sp^2 or sp^3 carbon for coupling.

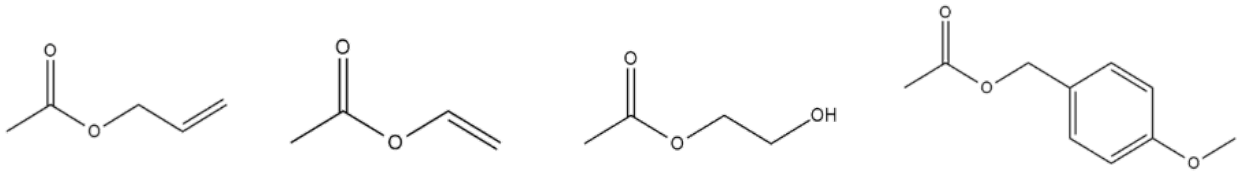

Allyl Acetate | Vinyl Acetate | 2-hydroxyethyl acetate | 4-methoxybenzyl acetate

Scheme 3. Structure of the neutral acetate esters used for the ion molecule reaction with $[(phen)Ni(R)]^+$

Vinyl acetate has a sp^2 reacting carbon atom. 2-hydroxyethyl acetate provides an –OH functionality in the R' group, while 4-methoxybenzyl acetate contains an ether functionality. Thus, the interaction of the three initial carboxylates (acetate, acrylate, and benzoate) and the four esters, combine to a total of 12 different reaction pairs.

As an exemplar, Figure 1 shows the reaction between $[(phen)Ni(C_6H_5)]^+$, *m/z* 315 (produced via decarboxylation of $[(phen)Ni(OOCC_6H_5)]^+$complex) and allyl acetate. Consistent with previous studies,[24] the only product of this reaction is the displacement of the phenyl moiety in the

organonickel species by the acetate resulting in $[(phen)Ni(OOCCH_3)]^+$, *m/z* 297 (P_i), accompanied by the elimination of allyl benzene.

When one starts with the acetate ternary complex, the C-C coupling reaction results in completing the catalytic cycle (Scheme 1) with regenerating the initial acetate complex $[(phen)Ni(OOCCH_3)]^+$ in the process.

Although we did not measure the reaction kinetics, the reactions of all organonickel ions with the esters were very fast, appearing to be close to the collision rate, except for 4-methoxybenzyl acetate. Reactions with 4-methoxybenzyl acetate did not produce product ions at the similarly high rate, but we believe this was not due to the lower rate constant but rather due to the very low volatility of this ester affecting its pressure inside the ion trap. In either case, the reaction was sufficiently fast to form the product ions in measurable quantities.

All 12 possible combinations of the three initial carboxylates and the four esters resulted in C-C coupling reactions with all coupling products shown in Scheme 4.

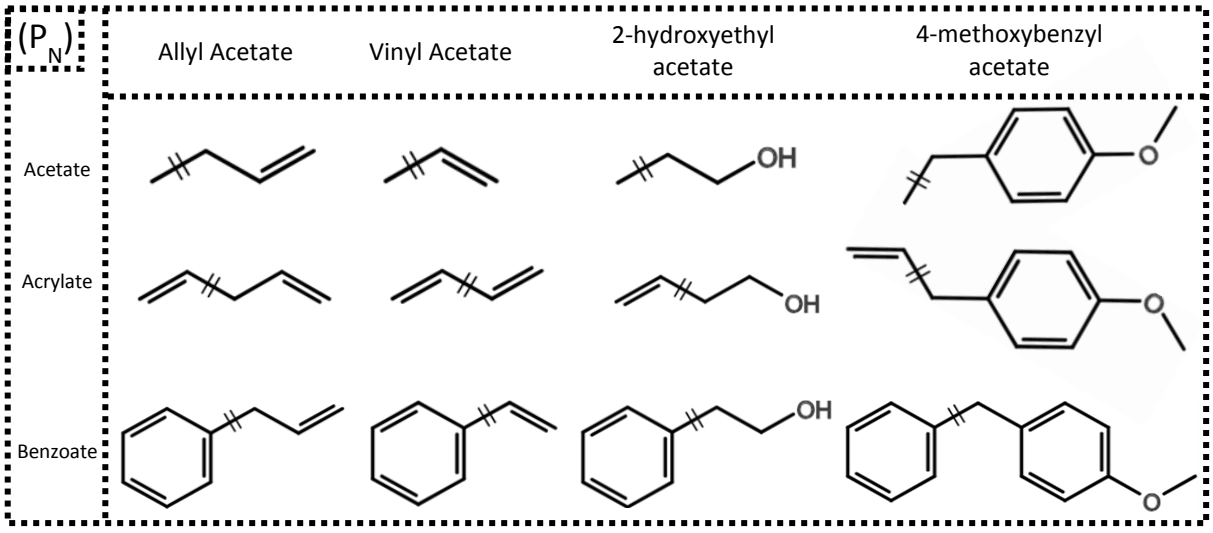

Scheme 4. C-C coupling products formed in the ion-molecule reactions between $[(phen)Ni(R)]^+$ and the ester CH_3COOR' (eq. 1b).

Neutral 2-hydroxyethyl acetate produced very little C-C coupling products (0.5 – 2.5%), but instead underwent facile C-H coupling reactions (eq. 3):

$$[(phen)Ni(R)]^+ + CH_3COOCH_2CH_2OH \rightarrow [(phen)Ni(OCH_2CH_2OCOCH_3)]^+ + R\text{-}H \quad (3)$$

Thus, the nickel methyl complex eliminated methane, while nickel phenyl complex formed benzene. In addition, adduct ions of $[(phen)Ni(R)]^+$ and $CH_3COOCH_2CH_2OH$ were observed. The identity of these ions is discussed below. The C-H coupling is an expected outcome for the reaction of organometallic compounds and acids such as water and alcohols [25].

Our findings show that the C-C coupling reactions in the gas phase are not strongly affected by the character of the carbon (sp^3, sp^2, or aromatic). It also does not seem to matter whether these types of substituents appear at the organometallic side of the equation (carrying a partially negative charge), or as the ester R' groups (thus carrying a partially positive charge). It is also

encouraging to note that the ether functional group do not seem to hamper the C-C coupling process.

Analysis of the C-C coupling reaction energetics

Previous studies have identified various potential mechanisms for the C-C bond coupling reactions of organonickel(II) complexes reacting with allyl acetate that range from oxidative addition- reductive elimination pathways through to alkene insertion followed by β-acetate transfer .[11,26] A common feature for all of the reaction pathways is the formation of reactant (R_I + R_N) and product complexes (P_I +P_N). Given the diversity of acetate esters examined experimentally, a detailed DFT study of all reactions manifolds is beyond the scope of this study. Rather, to investigate these C-C coupling reactions, we have focussed on characterizing the separated reactants (R_I) + (R_N), reactant complexes (R_I + R_N), product complexes (P_I) + (P_N) and separated products (P_I +P_N) computationally at the M11L/cc-pVTZ level of theory. Figure 3 shows the calculated geometries of these combinations for the reaction between $[(phen)Ni(CH_3)]^+$and vinyl acetate. Full computed energetics for all 12 C-C coupling reactions are given in Table 1. Formation of the ion-molecule reactant complex (R_I+R_N) (see Fig. 3b) is exothermic (compared to the separated reactants R_I and R_N) by 91-167 kJ/mol depending on the system. The fact that the coupling reaction occurs experimentally, suggests that there is a reaction pathway that proceeds via one or more transition states that have barriers below the energy of the separated reactants (which we did not attempt to calculate these). Once C-C coupling has formed, another ion-molecule complex (P_I+P_N) is formed, this time between the products, which is shown in Fig. 3c. This second complex represents the lowest energy point on the reaction coordinate, and is exothermic by 160-213 kJ/mol. The last step is the separation of the product ion-molecular product complex, (P_I+P_N), into individual components P_I (ion) and P_N (neutral), which are pictured as (P_I) + (P_N) in Fig. 3d. This step is slightly endothermic, 22 –53 kJ/mol. Ions in the ion trap certainly have enough energy to overcome this level of

endothermicity, but it can explain why in addition to the separated products the ion-molecule product complex is also detectable in most reactions. Overall, all coupling reactions described by eq. 1b are exothermic by 246 – 285 kJ/mol (Table 1). Among the three carboxylates, acetate produces the most exothermic coupling, followed by benzoate and then acrylate.

In most of the experimental ion-molecule reaction spectra leading to C-C coupling, in addition to the regeneration of the $[(phen)Ni(OOCR)]^+$ species, an extra product peak appeared with an *m/z* corresponding to the addition of the neutral ester to the reactant ion $[(phen)Ni(R)]^+$, as shown in Fig. 4. It is not immediately clear whether this peak is an adduct of the reactant ion and neutral, (R_I+R_N), or an ion-molecule complex of the ionic and neutral products, (P_I+P_N), since these two species are isobaric. For example, in Fig. 4 the ion at *m/z* 365 (adduct of the $[(phen)Ni(CH=CH_2)]^+$ ion and the neutral allyl acetate) can be $\{[(phen)Ni(R^1)]^+ + CH_3COO(R^2)\}$ which we designate (R_I+R_N), or $\{[(phen)Ni(OOCCH_3)]^+ + R^1\text{-}R^2\}$ which we will label as (P_I+P_N).

To probe the identity of this ion, it was mass-selected and subjected to CID. The fragmentation resulted exclusively in $[(phen)Ni(OOCCH_3)]^+$ at *m/z* 297 (Figure S1). Furthermore, the CID amplitude required to dissociate the complex was very low. These findings strongly suggest that the ion *m/z* 365 in Fig. 4 is the loosely bound product complex (P_I+P_N). This was found to be true for reactions with allyl acetate and vinyl acetate. Reactions of 4-methoxybenzyl acetate were not monitored long enough to observe the adduct.

The situation was different for the ion-molecule reactions with 2-hydroxymethyl acetate. This neutral formed mostly the adduct (base peak), and upon CID the adduct returned the reactant ion $[(phen)Ni(R)]^+$ and neutral 2-hydroxymethyl acetate, in addition to the C-H coupling products which were described above. Thus, it seems that for this neutral the adduct is the (R_I+R_N) ion-molecule complex. It is not clear why the (R_I+R_N) complex of 2-hydroxymethyl acetate is

trapped, but the answer may lie in the higher-energy TS for going from (R_I+R_N) to (P_I+P_N) due to extra hydrogen-bonding possibilities available to 2-hydroxymethyl acetate.

Previous studies have shown that ternary organonickel complex cations, $[(L)Ni(R)]^+$, can exist in a lower-energy triplet state depending on the ligand, L.[27] To investigate this possibility, we calculated the relative energy of $[(phen)Ni(R)]^+$ and $[(phen)Ni(OOCR)]^+$ ions in both singlet and triplet states at the M06L/6-311+G(d,p) level of theory. For the carboxylate complexes, the singlet state was substantially lower in energy (~70 kJ/mol for acetate, acrylate, and benzoate). The organometallic nickel species $[(phen)Ni(R)]^+$ with R = phenyl or vinyl were also lower in energy as singlets, by 38 and 51 kJ/mol, respectively. Only for $[(phen)Ni(CH_3)]^+$ is the triplet lower in energy, but only by 2 kJ/mol. Given the fairly high values of ΔH°_{298} for reactions (1b) (Table 1), this small triplet energy advantage for the Ni-methyl complex should not affect our assignments significantly.

Conclusions

Previous reports of gas-phase C-C coupling reactions focused on coupling simple moieties (methyl, allyl, phenyl). In this work, we show that Ni(II)-phenanthroline-catalyzed coupling reactions can be performed with a variety of carbon substituents (sp^3, sp^2, or aromatic), some of them with ether-functional groups. Reaction rates do not seem to be strongly dependent on the nature of the substituents, as sp^3 - sp^3 or sp^2- sp^2 coupling reactions all proceed rapidly.

The fact that ether moiety does not hinder C-C coupling process is very encouraging. We will continue working on expanding this method to other functionalities. Not every functional group will work, however, as shown for halogen-substituted carboxylates, which do not lose CO_2 to yield organonickel species under CID conditions (eq. 1a). Furthermore, substrates containing

labile hydrogen atoms (such as alcohols explored in this work) may react via C-H bond formation instead of the desired C-C coupling reaction (eq. 1b).

While there have been many impressive advances in sp^2–sp^3 and sp^3–sp^3 couplings recently, additional methodologies to enable C-C coupling reactions across a broader range of potential scaffolds are highly desired[6]. This work shows that using Ni-based catalysts in the CO_2ExR type of reaction can be promising for making new coupling products.

Acknowledgments

This work has been supported in part by the Department of Chemistry and Biochemistry, Northern Illinois University. Acknowledgment is made to the Donors of the American Chemical Society Petroleum Research Fund (PRF # 59763-ND6) for partial support of this research. RAJO thanks the Australian Research Council for financial support DP180101187.

References

1. C. C. C. Seechurn, M. O. Kitching, T. J. Colacot, V. Snieckus. Palladium-Catalyzed Cross-Coupling: A Historical Contextual Perspective to the 2010 Nobel Prize. *Angew. Chem. Int. Ed.* **2012**, 51 (21), 5062–5085..
2. Ananikov, V. P. Nickel: The "Spirited Horse" of Transition Metal Catalysis. *ACS Cat.* **2015**, 5 (3), 1964–1971.
3. K. Eller, H. Schwarz, Organometallic Chemistry in the Gas Phase. *Chem. Rev.* **1991**, 91 (6), 1121–1177.
4. H. Schwarz. Remote Functionalization of C-H and C-C Bonds by "Naked" Transition-Metal Ions (Cosi Fan Tutte). *Acc. Chem. Res.* **1989**, 22 (8), 282–287
5. M. Schlangen, H. Schwarz, Effects of Ligands, Cluster Size, and Charge State in Gas-Phase Catalysis: A Happy Marriage of Experimental and Computational Studies. *Cat. Let.* **2012**, 142 (11), 1265–1278.
6. D. Schroder, H. Schwarz, Gas-Phase Activation of Methane by Ligated Transition-Metal Cations. *PNAS* **2008**, 105 (47), 18114–18119
7. H. Schwarz, Metal-Mediated Activation of Carbon Dioxide in the Gas Phase: Mechanistic Insight Derived from a Combined Experimental/Computational Approach. *Coord. Chem. Rev.* **2017**, 334, 112–123.
8. D. K. Böhme, H. Schwarz. Gas-Phase Catalysis by Atomic and Cluster Metal Ions: The Ultimate Single-Site Catalysts. *Angew. Chem. Int. Ed.* **2005**, 44 (16), 2336–2354.
9. R. A. J. O'Hair, N. J. Rijs. Gas Phase Studies of the Pesci Decarboxylation Reaction: Synthesis, Structure, and Unimolecular and Bimolecular Reactivity of Organometallic Ions, *Acc. Chem. Res.* **2015**, 48 (2), 329–340.
10. C. C. Le, D. W. C. Macmilla. Fragment Couplings via CO_2 Extrusion–Recombination: Expansion of a Classic Bond-Forming Strategy via Metallaphotoredox. *J. Am. Chem. Soc* 2015, 137 (37), 11938–11941.

11. M. Woolley, A. Ariafard, G.N. Khairallah, K. H. Y. Kwan, P.S. Donnelly, J.M. White, A.J. Canty, B.F. Yates, R.A.J. O'Hair. Decarboxylative-Coupling of Allyl Acetate Catalyzed by Group 10 Organometallics, [(Phen)M(CH_3)]. *J. Org. Chem.*2014, 79 (24), 12056–12069

12. D. C. Blakemore, L. Castro, I. Churcher, D.C. Rees, A.W. Thomas, D.M. Wilson, A. Wood. Organic Synthesis Provides Opportunities to Transform Drug Discovery. *Nature Chem.* **2018**, 10 (4), 383–394.

13. M. L. Parker, S. Gronert. Investigating Reduced Metal Species via Sequential Ion/Ion and Ion/Molecule Reactions: The Reactions of Transition Metal Phenanthrolines with Allyl Iodide. *Int. Jour. Mass Spec.* **2017**, 418, 73–78.

14. R. Peverati, D.G. and Truhlar. (2014) Quest for a universal density functional: the accuracy of density functionals across a broad spectrum of databases in chemistry and physics. *Phil. Trans. Roy. Soc. A: 372*, 20120476–20120476.

15. Gaussian 09, Revision A.02, M. J. Frisch, G. W. Trucks, H. B. Schlegel, G. E. Scuseria, M. A. Robb, J. R. Cheeseman, G. Scalmani, V. Barone, G. A. Petersson, H. Nakatsuji, X. Li, M. Caricato, A. Marenich, J. Bloino, B. G. Janesko, R. Gomperts, B. Mennucci, H. P. Hratchian, J. V. Ortiz, A. F. Izmaylov, J. L. Sonnenberg, D. Williams-Young, F. Ding, F. Lipparini, F. Egidi, J. Goings, B. Peng, A. Petrone, T. Henderson, D. Ranasinghe, V. G. Zakrzewski, J. Gao, N. Rega, G. Zheng, W. Liang, M. Hada, M. Ehara, K. Toyota, R. Fukuda, J. Hasegawa, M. Ishida, T. Nakajima, Y. Honda, O. Kitao, H. Nakai, T. Vreven, K. Throssell, J. A. Montgomery, Jr., J. E. Peralta, F. Ogliaro, M. Bearpark, J. J. Heyd, E. Brothers, K. N. Kudin, V. N. Staroverov, T. Keith, R. Kobayashi, J. Normand, K. Raghavachari, A. Rendell, J. C. Burant, S. S. Iyengar, J. Tomasi, M. Cossi, J. M. Millam, M. Klene, C. Adamo, R. Cammi, J. W. Ochterski, R. L. Martin, K. Morokuma, O. Farkas, J. B. Foresman, and D. J. Fox, Gaussian, Inc., Wallingford CT, 2016.

16. T. Sperger, I. A. Sanhueza, I. Kalvet, F. Schoenebeck Computational Studies of Synthetically Relevant Homogeneous Organometallic Catalysis Involving Ni, Pd, Ir, and

Rh: An Overview of Commonly Employed DFT Methods and Mechanistic Insights *Chem. Rev.*, **2015**, *115* (17), pp 9532–9586

17. G. L. Miessler, P. J. Fischer, D.A. Tarr, Inorganic chemistry *Pearson Boston*. **2014**
18. N. A. Eckert, A. Dinescu, T. R. Cundari, P. L. Holland. A T-Shaped Three-Coordinate Nickel(I) Carbonyl Complex and the Geometric Preferences of Three-Coordinate d9 Complexes, *Inorg. Chem.*, **2005**, 44, 7702–7704
19. P. L. Holland, T. R. Cundari, L. L. Perez, N. A. Eckert, R. J. Lachicotte, Electronically Unsaturated Three-Coordinate Chloride and Methyl Complexes of Iron, Cobalt, and Nickel, *J. Am. Chem. Soc*. **2002**, 124, 14416-14424.
20. M. Brookhart, M. L. Green. Carbon-hydrogen-transition metal bonds. *J. Organom. Chem*. *1983 250*, 395–408.
21. M. Brookhart, M. L. Green, G. Parkin. Agostic interactions in transition metal compounds. *PNAS* **2007** *104*, 6908–6914.
22. N.J. Rijs, R. A. J. O'Hair. "Forming Trifluoromethylmetallates: Competition Between Decarboxylation and C-F bond Activation of Group 11 Trifluoroacetate complexes, $[CF_3CO_2ML]^-$", *Dalton Trans*., **2012**, *41*, 3395 – 3406
23. H. Al Sharif, K. L. Vikse, G. N. Khairallah, R. A.J. O'Hair. Catalytic Decarboxylative Coupling of Allyl Acetate: Role of the Metal Centers in the Organometallic Cluster Cations $[CH_3Cu_2]^+$,$[CH_3AgCu]^+$, and $[CH_3Ag_2]^+$. *Organometallics* **2013,** *32* (19), 5416-5427.
24. N. J. Rijs, R.A.J. O'Hair. Dimethylcuprate-catalyzed decarboxylative coupling of allyl acetate. *Organometallics* **2012,** *31* (22), 8012-8023;
25. M. Woolley, G. N. Khairallah, G.D. Silva, P.S. Donnelly, R.A.J. O'Hair. Direct versus Water-Mediated Protodecarboxylation of Acetic Acid Catalyzed by Group 10 Carboxylates, $[(Phen)M(O_2CCH_3)]$. *Organometallics* **2014**, 33 (19), 5185–5197.
26. K. L. Vikse, G.N. Khairallah, A. Ariafard, A.J. Canty, R.A. J. O'Hair. Gas-Phase and Computational Study of Identical Nickel and Palladium Mediated Organic

Transformations where Mechanisms Proceeding via M^{II} or M^{IV} Oxidation States are Determined by Ancillary Ligands. *J. Am. Chem. Soc.*, **2015**, *137*, 13588–13593

27. M. Schlangen, H. Schwarz. Ligand Effects on the Mechanisms of Thermal Bond Activation in the Gas-Phase Reactions NiX /CH_4→Ni(CH_3) /HX (X=H, CH_3, OH, F). Short Communication. *Helv. Chim. Act*. **2008**, 91 (12), 2203–2210.

R= Acetate			**R= Benzoate**			**R= Acrylate**		
ΔH^0_{298} $(P_I)+(P_N)$	ΔH^0_{298} $(R_I + R_N)$	ΔH^0_{298} $(P_I + P_N)$	ΔH^0_{298} $(P_I)+(P_N)$	ΔH^0_{298} $(R_I + R_N)$	ΔH^0_{298} $(P_I + P_N)$	ΔH^0_{298} $(P_I)+(P_N)$	ΔH^0_{298} $(R_I + R_N)$	ΔH^0_{298} $(P_I + P_N)$
kJ/mol	kJ/mol	kJ/mol	kJ/mol	kJ/mol	kJ/mol	kJ/mol	kJ/mol	kJ/mol

Table 1

Values of ΔH^{o}_{298} for the main species relative to the energy of the separated reactants ($(R_I)+(R_N)$), calculated at the M11L/cc-pVTZ level of theory.

Vinyl acetate	-277	-127	-299	-264	-126	-308	-259	-91	-304
Allyl acetate	-285	-151	-309	-262	-133	-304	-247	-98	-275
2-hydroxyethyl acetate	-284	-158	-313	-262	-135	-306	-246	-94	-281
4-methoxybenzyl acetate	-284	-167	-337	-261	-156	-313	-248	-112	-301

List of tables

Table 1.

Values of $\Delta H°_{298}$ for the main species relative to the energy of the separate reactants ($(R_I)+(R_N)$), calculated at the M11L/cc-pVTZ level of theory.

List of figures

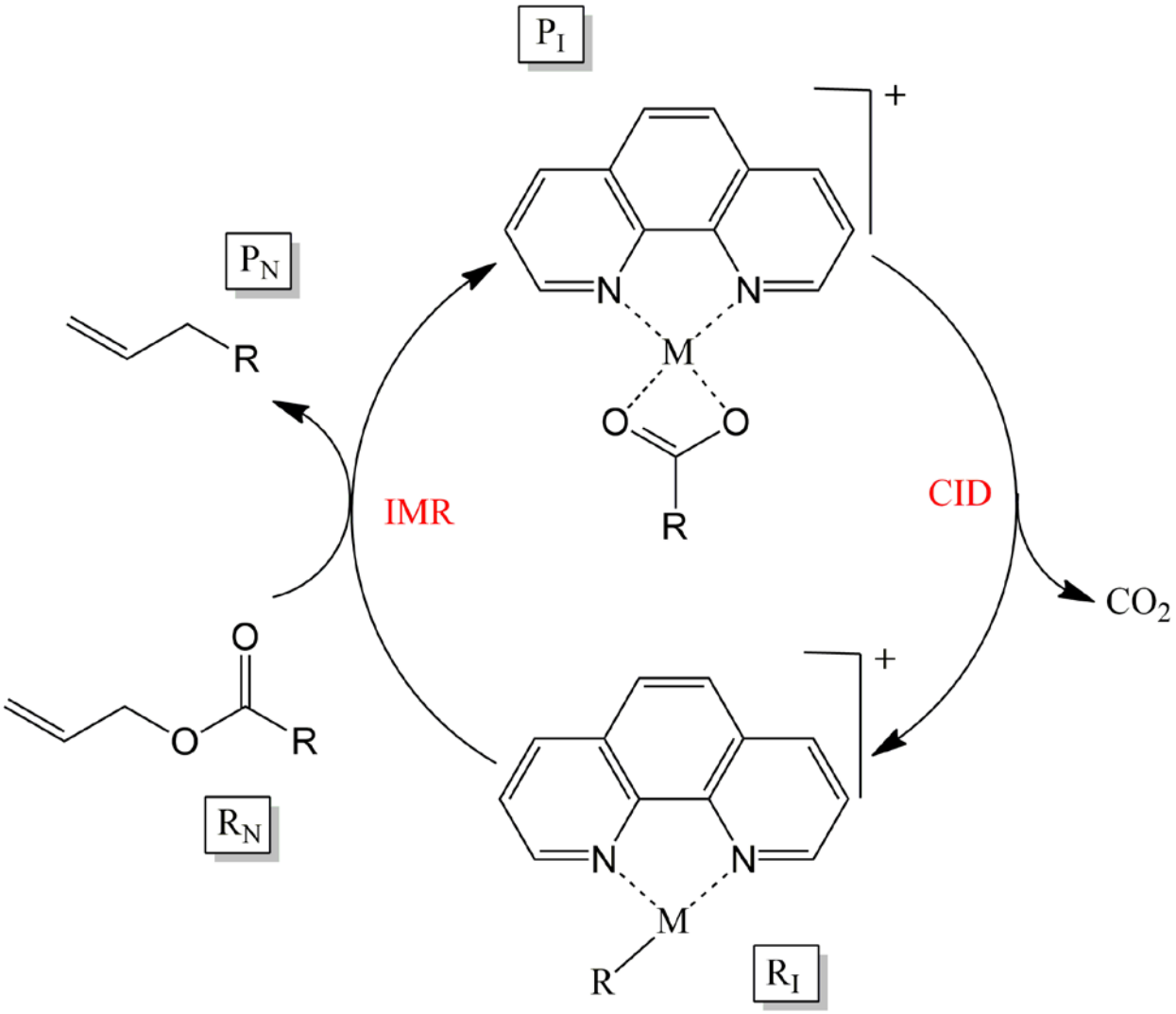

Scheme 1.

Two-step catalytic cycle for the gas-phase CO_2ExR C-C coupling reaction involving CID loss of CO_2 (eq. 1a) followed by IMR with the ester (eq. 1b).

Figure Top

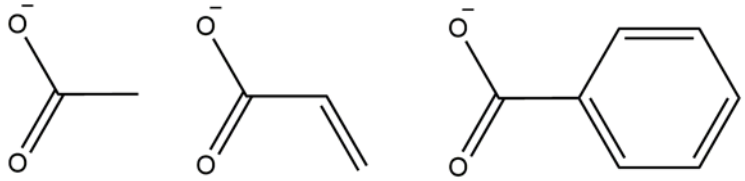

Scheme 2.

Structures of the carboxylates used in this work.

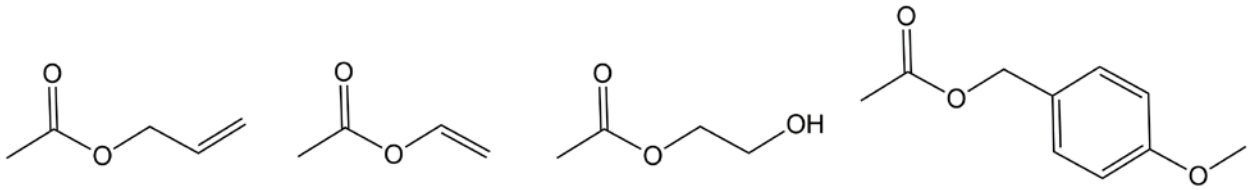

allyl acetate vinyl acetate 2-hydroxyethyl acetate 4-methoxybenzyl acetate

Scheme 3. Structure of the neutral acetate esters used for the ion molecule reaction with $[(phen)Ni(R)]^+$

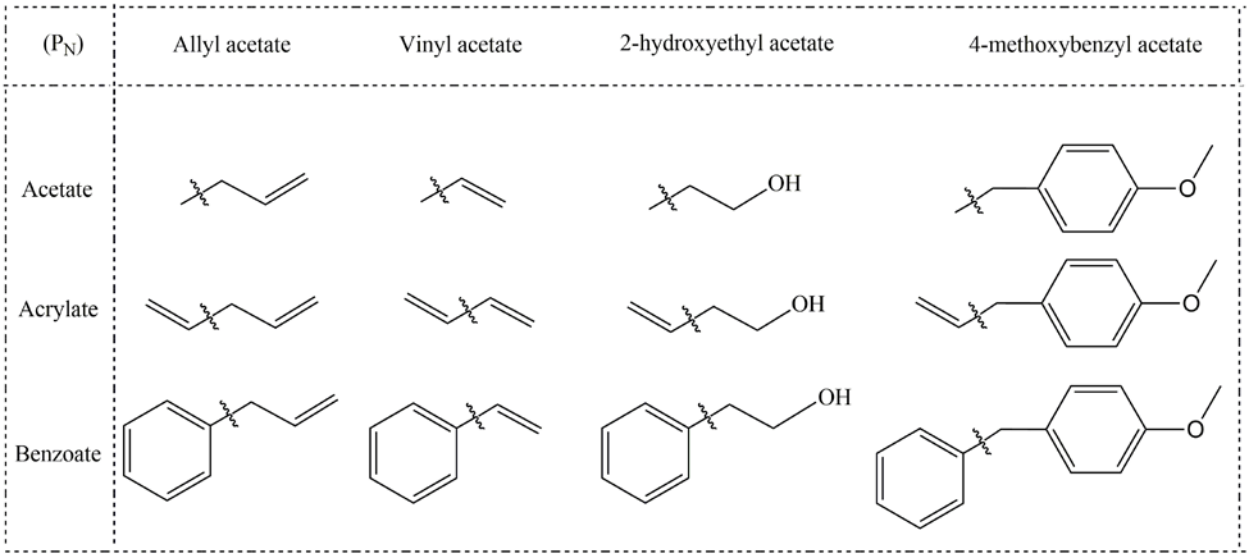

Scheme 4. C-C coupling products formed in the ion-molecule reactions between $[(phen)Ni(R)]^+$ and the ester CH_3COOR' (eq. 1b).

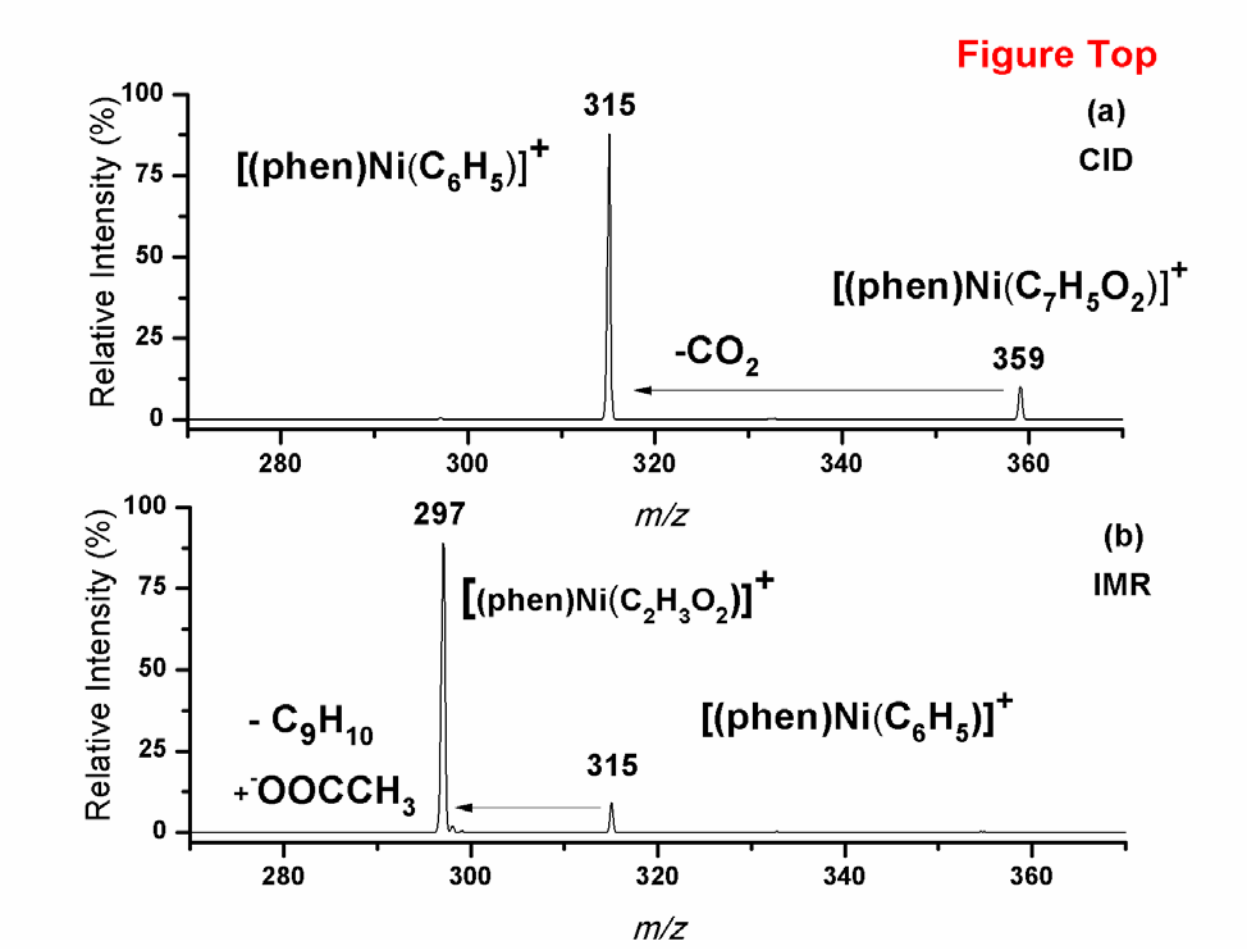

Figure 1.

(a) CID of $[(phen)Ni(C_7H_5O_2)]^+$ at *m/z* 359 showing loss of CO_2 to generate *m/z* 315, followed by (b) IMR with allyl acetate. Generation of $[(phen)Ni(C_2H_3O_2)]^+$ at *m/z* 297 indicates C-C bond coupling.

Figure Top

Figure 2.

Organometallic ion $[(phen)Ni(R)]^+$ geometries for R=methyl (a), vinyl (b), and phenyl (c) optimized at the M11L/cc-pVTZ level of theory.

Figure Top

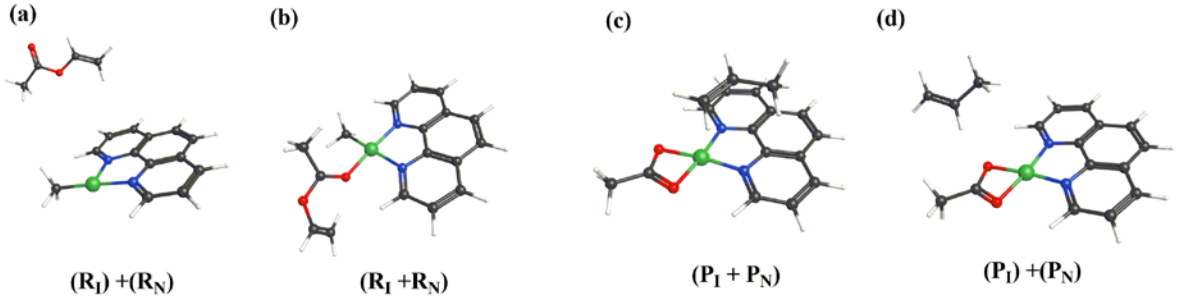

Figure 3.

Possible structures of the IMR adduct product for the reaction of $[(phen)Ni(CH_3)]^+$ (R_I) reacting with vinyl acetate (R_N). (a) separated reactants; (b) ion-molecule complex of the neutral reactant and the organometallic ion (R_I +R_N); (c) ion-molecule complex between the products, (P_I+P_N); (d) separated products.

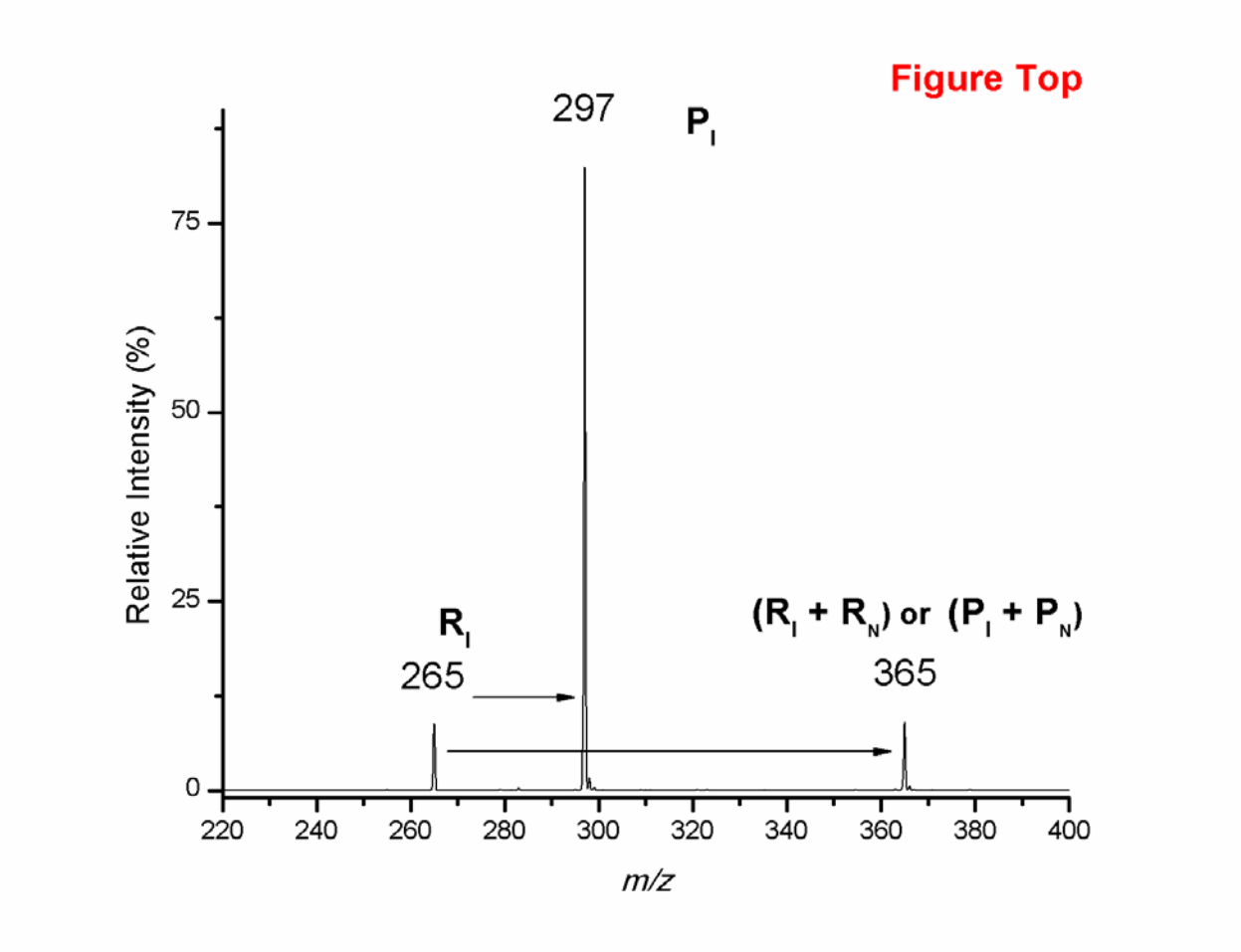

Figure 4.

Scan at 100 ms reaction time between $[(phen)Ni(CH{=}CH_2)]^+$ and allyl acetate (R_N). The product peak $[(phen)Ni(CH_3COO)]^+$ (P_I) at *m/z* 297 is observed along with a side product (R_I+R_N) or (P_I+P_N) at *m/z* 365.

Figure Top

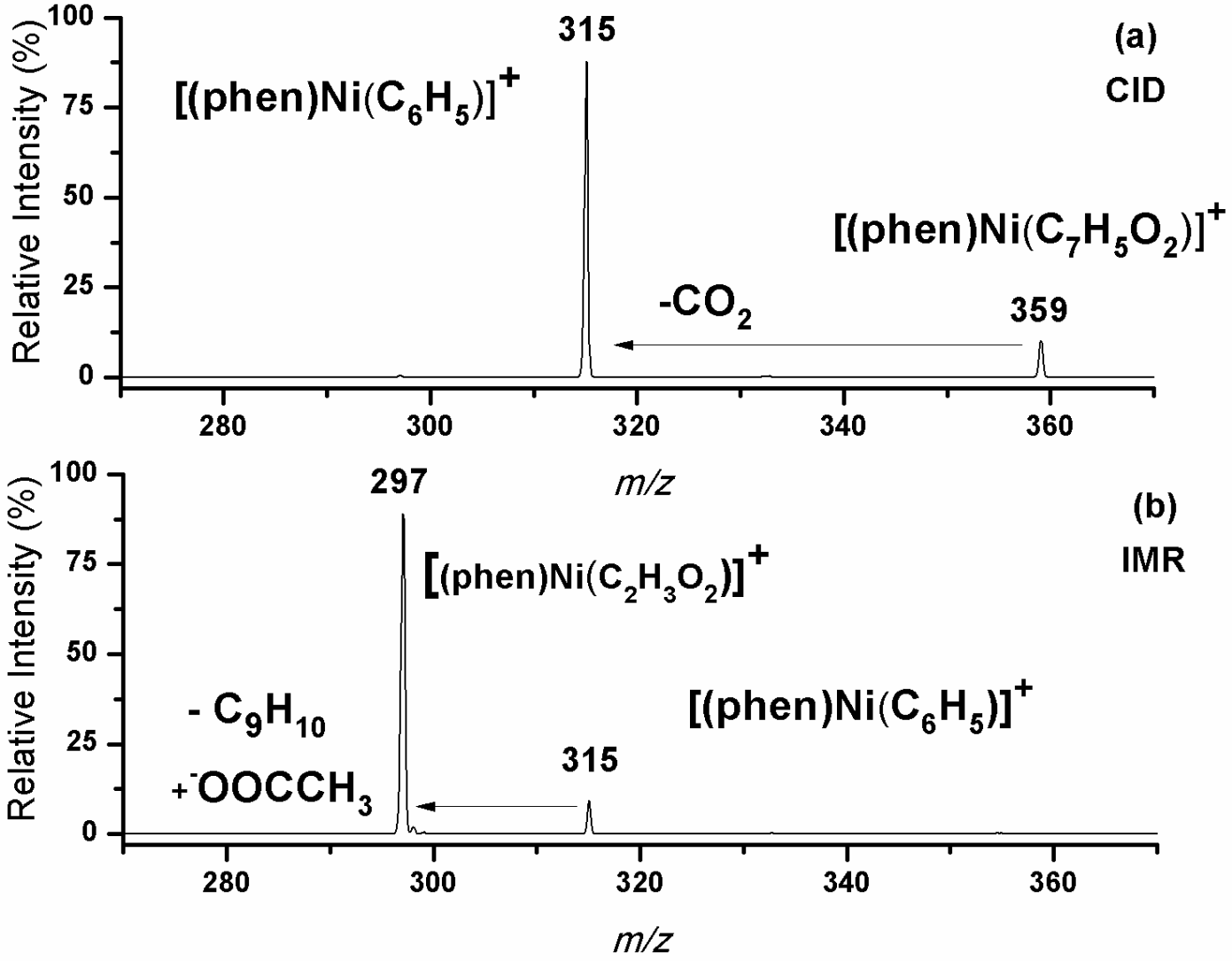

JMS_4360_Figure 1.tif

Figure Top

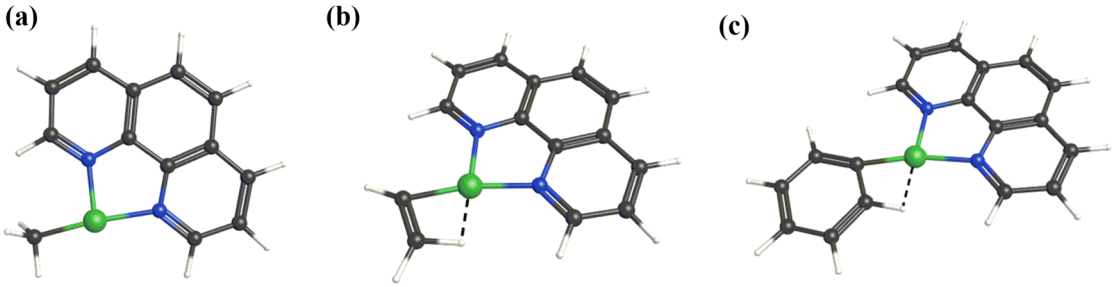

JMS_4360_Figure 2.tif

Figure Top

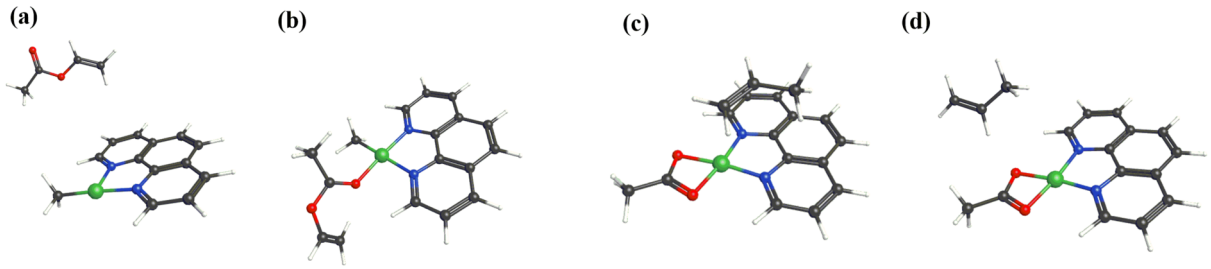

JMS_4360_Figure 3.tif

Figure Top

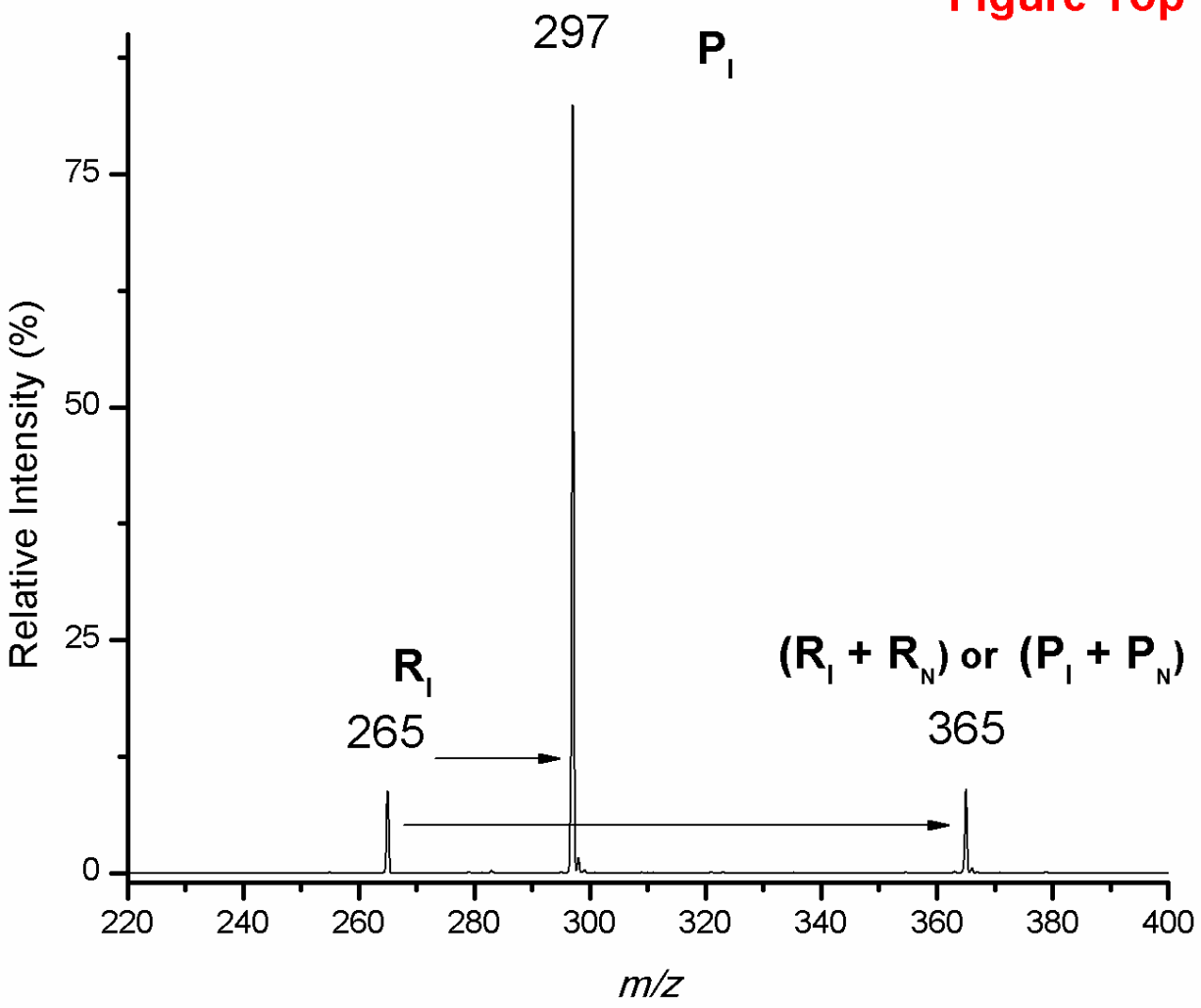

JMS_4360_Figure 4.tif

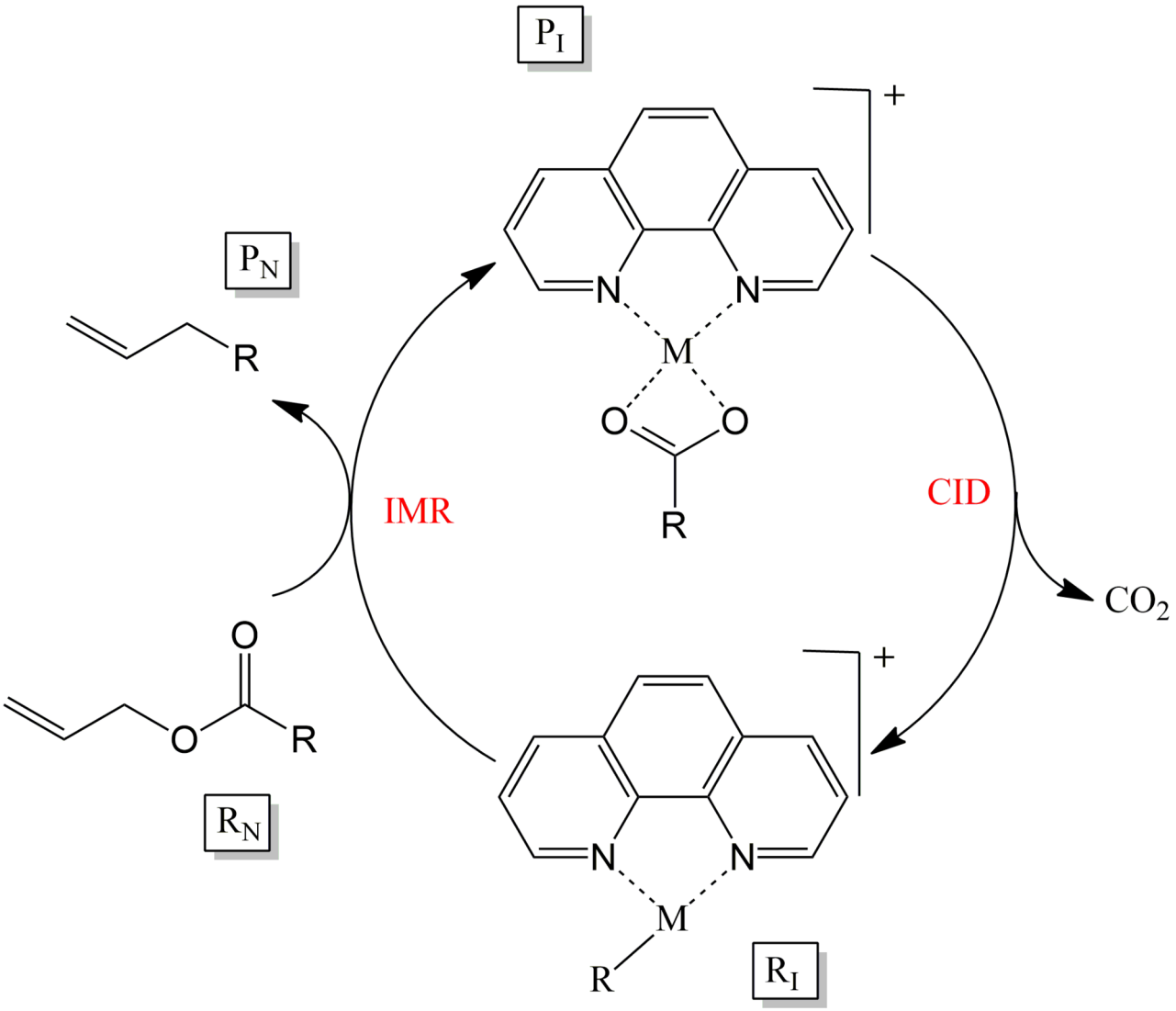

JMS_4360_Scheme 1.tif

Figure Top

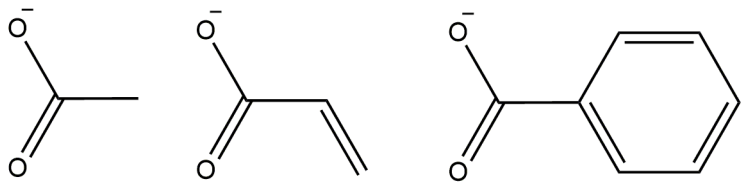

JMS_4360_Scheme 2 .tif

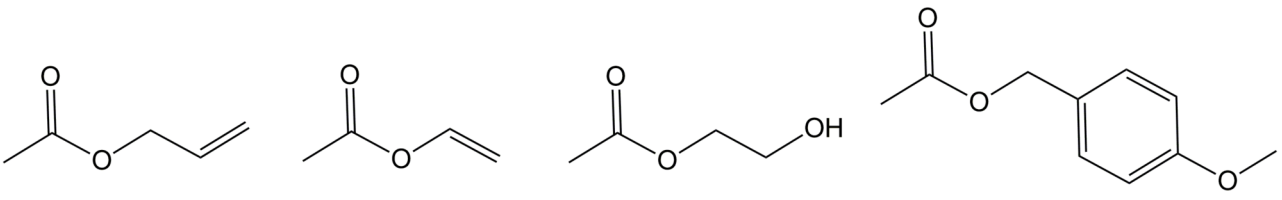

JMS_4360_Scheme 3.tif

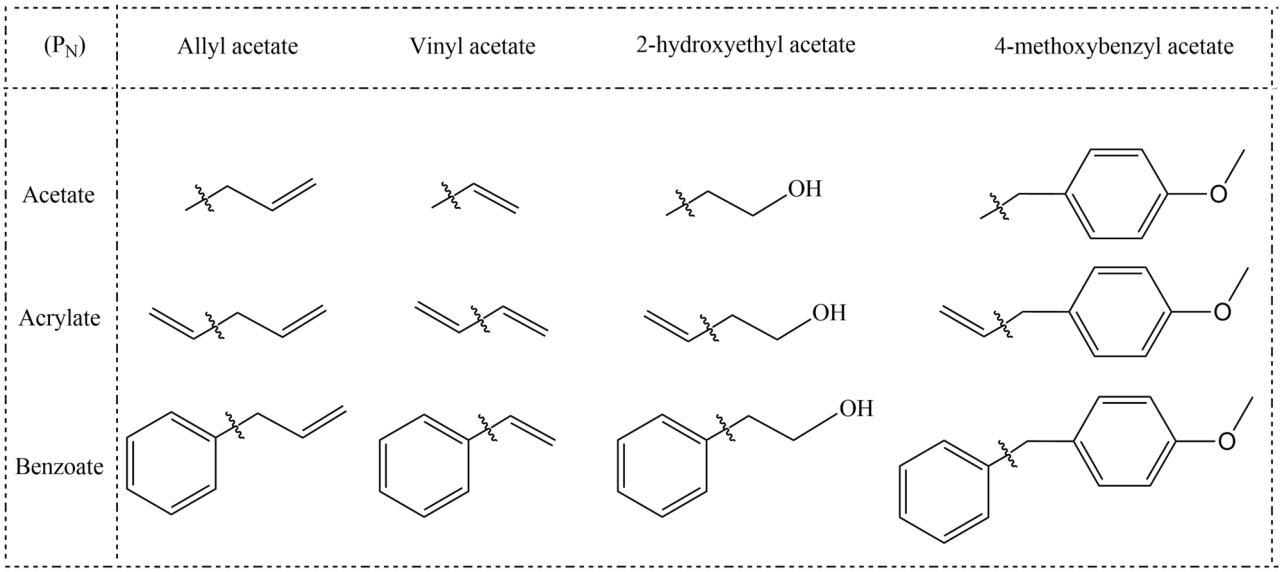

JMS_4360_Scheme 4.tif